Journal of Computation Physics and Earth Science
ISSN: 2776-2521 (online)
Volume 6, Number 1, April 2026, Page 7 - 13
https://journal.physan.org/index.php/jocpes/index

Epicenter and Hypocenter Determination Using the Grid Search Method for the 5 August 2018 Lombok Earthquake

Qisthi Mursyida[1]
[1]College of Meteorology, Climatology, and Geophysics

Article Info

Article history:

Received December 30, 2025
Revised January 15, 2026
Accepted March 10, 2026

Keywords:

Grid search method
Lombok earthquake 2018
Epicenter
Hypocenter
P-wave arrival time
RMS misfit

A B S T R A C T

The Lombok Island region is characterized by complex tectonic interactions associated with the subduction of the Indo-Australian Plate beneath the Sunda Plate and the activity of th Flores Back Arc Thrust, resulting in frequent moderate to large earthquakes. One of the most significant events in this region is the Mw 7.0 Lombok earthquake that occurred on 5 August 2018. Accurate determination of the earthquake epicenter and hypocenter is essential for understanding the source characteristics and regional seismotectonic setting. Grid search method was applied to determine the epicenter and hypocenter of the 5 August 2018 Lombok earthquake using P-wave arrival time data revorded by 15 accelerometer. The method evaluates a 3D spatial grid by calculating thereotical travel times based on a homogeneous P-wave velocity model and minimizing the MRS residual between observed and calculated arrivals, yielding a best fit location at latitude −8.2483°, longitude 116.5566°, focal depth of 39.00 km, and a minimum RMS of 1.0064 . Comparison with the BMKG earthquake catalog shows good agreement in apicenter location and focal depth, while RMS based analyses indicate that the earthquake location is well constrained both horizontally and vertically.

Corresponden Author:

Qisthi Mursyida,
College of Meteorology, Climatology, and Geophysics
Tangerang, Indonesia
Email: mursyidaq@gmail.com

1. INTRODUCTION

Indonesia is one of the most seismically active countries in the world due to its complex tectonic setting. The Indonesian archipelago is located at the convergence of three major tectonic plates, Eurasian Plate, Indo-Australian Plate, and the Pacific Plate. This tectonic interaction places Indonesia within the circum Pacific seismic belt, commonly referred to as the Ring of Fire, which is characterized by intense seismic and volcanic activity [1]. The relative motion of these plates generates various tectonic structures, including subduction zones, crustal fault systems, and back-arc thrust, which significantly increase the occurrence of destructive earthquakes throughout the region.

One of the regions strongly affected by this tectonic interaction is the Lesser Sunda Islands, including Lombok Island. Seismicity in this area is primarily controlled by the northward subduction of the Indo-Australian Plate beneath the Sunda Plate along the Sunda Trench, as well as the activity of the Flores Back-Arc Thrust located to the north of Lombok. This tectonic configuration has produced frequent moderate to large earthquakes, including the Lombok earthquake sequence in 2018, which resulted in severve damage and significant societal impacts [2].

The mainshock that occured on 5 August 2018 (Mw 7.0) represents one of the most significant seismic events in the Lombok earthquake sequence. Accurate determination of the epicenter and hypocenter of this earthquake is crucial of understanding the earthquake source mechanism, fault geometry, and regional seismotectonic characteristics. Hypocenter location plays a fundamental role in distinguishing whether an earthquake is associated with subduction processes, shallow crustal faulting, or back-arc thrust activity [3].

Various method have been developed to determine earthquake epicenter and hypocenter locations, ranging from linearized inversion techniques to probabilistic and nonlinear approaches. In tectonically complex regions such as Indonesia, however, the reliability of conventional linearized methods is often reduced due to strong lateral velocity heterogeneity, uneven seismic station distribution, and uncertainties in seismic phase arrival times [4]. These factors may lead to biased solutions and poorly constrained hypocentral depths, particularly for earthquake occuring in offshore or back-arc settings.

An alternative approach to overcome these limitations is the grid search method, which is a direct forward-modelling technique that systematically evaluates a predefined 3d spatial grid. For each grid node, theoretical travel times are calculated using an assumed velocity model and compared with observed arrival times, and the optimal earthquake location is determined by minimizing a misfit function, commonly expressed as the root mean square (RMS) or travel time residuals [5]. Unlike linearized inversion methods, the grid search approach does not require an initial starting model and is less susceptible to convergence toward local minima, making it particularly suitable for regions with complex tectonic settings and limited station coverage. In this study, the grid search method is applied to determine the epicenter and hypocenter of the Mw 7.0 Lombok earthquake that occurred on 5 August 2018. By systematically exploring the spatial distribution of RMS misfit values, this approach allows for a robust assessment of location uncertainty.

2. RESEARCH METHOD

This study uses seismic data recorded by 15 accelerometer stations distributed around Lombok Island and its surrounding regions, covering a geographic area approximately bounded by longitude 112.5°–120.5°E and latitude 9.7°–5.0°S. The distribution of the accelerometer stations, including their geographic coordinates and arrival time, is summarized in Tabel 1. The dataset corresponds to the mainshock of the Lombok earthquake sequence that occurred on 5 August 2018 (Mw 7.0). The accelerometer records provide high quality waveform data suitable for precise arrival time analysis, particularly for strong ground motion events. P-wave arrival times were obtained through an automatic picking (autopicking) process applied to the recorded waveforms. To ensure the reliability of the arrival time data, the autopicking results were subsequently subjected to a quality control (QC) procedure conducted by the researchers. This QC process involved visual inspection any correction of the picked P-wave onsets to minimize picking errors and to ensure consistency across all stations. Only P-wave arrivals that satisfied the quality criteria were included in the subsequent location analysis.

Table 1. Location of seismic stations and p-wave arrival times

Stasiun	Longitude	Latitude	Phase	*Arrival Time* (UTC)
BMNI	118.69269	-8.5427	P	11:47:12
DEBI	115.179	-8.738	P	11:47:00
DEMO	115.18	-8.74	P	11:47:00
ITSU	112.795715	-7.280119	P	11:47:37
JAGI	114.153261	-8.470653	P	11:47:12
JBJN	113.7174	-8.15565	P	11:47:19
LABA	119.886	-8.4866	P	11:47:28
MAKO	112.5975	-7.90112	P	11:47:35
NEKI	114.6174	-8.3408	P	11:47:05
PLAI	117.7765	-8.8273	P	11:47:00
RMNN	120.47801	-8.59793	P	11:47:36
SUBE	117.4135	-8.4879	P	11:46:53
SUHA	119.5449	-5.0589	P	11:47:41
TRES	112.6891	-7.664	P	11:47:34
WGNI	120.2976	-9.6692	P	11:47:36

The epicenter and hypocenter of the earthquake were determined using the grid search method, which is a forward modelling approach that systematically evaluates potential source locations within a predfined spatial grid. A 3d grid was constructed covering the study area, including horizontal coordinates and depth. For each grid node, theoretical P-wave travel times were calculated using a constant P-wave velocity model [6].

At each grid point with coordinates (X_0, Y_0, Z_0), the model P-wave arrival time (t_{model}) was calculated based on the geometric distance between the grid node and each seismic station, assuming a homogeneous velocity structure. The midel arrival time is expressed as:

$$t_{model} = t_0 + \frac{\sqrt{(X_0 - X_i)^2 + (Y_0 - Y_i)^2 + Z_0^2}}{V_p} \tag{1}$$

where X_i and Y_i represent the horizontal coordinates of the i-th station, Z_0^2 is the depth of the grid node, and V_p is the P-wave velocity. The origin time t_0 was estimated at each grid node as the average difference between the observed arrival times (t_{obs}) and the calculated travel times (t_{cal}).

The misfit between observed and theoretical arrival times was quantified using the RMS residual, defined as:

$$RMS = \sqrt{\frac{1}{N}\sum_{i=1}^{N}(t_i^{obs} - t_i^{cal})^2} \tag{2}$$

where t_i^{obs} and t_i^{cal} are the observed and calculated P-wave arrival times at the i-th station, respectively, and N is the total number of stations. The grid node corresponding to the minimum RMS value was selected as the best fit epicenter and hypocenter location. Compared to conventional inversion based methods, the grid search approach is not prone to convergence toward local minima and provides a more complete representation of the misfit landscape.

All data processing and analysis in this study were performed using Python. The procedur of the grid search method employed in this study is summarized in the flowchart sown in Figure 1. The workflow begins with the input of seismic waveform data and the definition of 3d spatial grid covering the study area. For each grid node, theoretical P-wave travel times are calculated and the RMS misfit between observed and calculated arrival times is evaluated. This process is repeated iteratively for all grid nodes to ensure exhaustive exploration of the model space. Once all grid points have been evaluated, the grid node associated with the minimum RMS value is selected as the best fit epicenter and hypocenter location. Finally, the distribution of RMS values is analyzed to assess the uncertainty and robustness of the obtained solution.

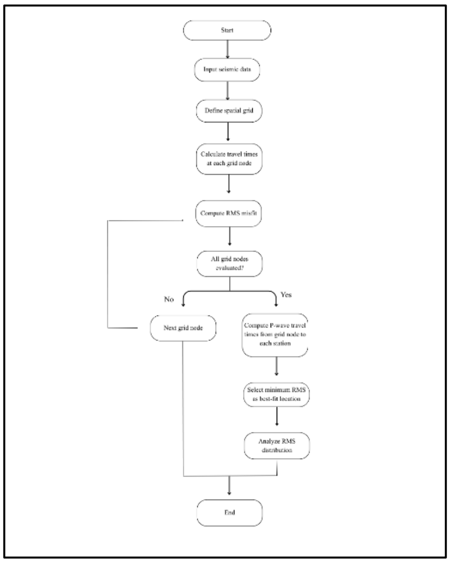

Fig. 1 Flowchart of the grid search method

3. RESEARCH METHOD

3.1. Earthquake Location Resultes and Validation

The epicenter location of the earthquake was determined using the grid search method based on P-wave arrival times recorded by 15 accelerometer stations. The grid search analuysis resulted in a best fit earthquake location with geographic coordinates:

a. Latitude : -8.2483
b. Longitude : 116.5566
c. Depth : 39.00 km
d. RMS : 1.0064

To evaluate the realibility of the obtained earthquake location, the grid search results were compared with the earthquake catalog by Indonesian Agency of Meteorology, Climatology, and Geophysics (BMKG), accessed through the WebDC BMKG platform. The comparison between the epicenter coordinates and focal depth derived in this study and those reported in the BMKG catalog in Table 2.

Table 2. Comparison of earthquake location parameters obtained from the grid search method and the BMKG catalog (WebDC BMKG)

Parameter	Grid Search Result	BMKG Catalog (WebDC)
Latitude (°)	-8.2483	-8.35
Longitude (°)	116.5566	116.47
Depth (km)	39.00	32.4

The comparison between the earthquake location parameters obtained from the grid search method and those reported in the BMKG catalog (WebDC BMKG), as presented in Table 2, shows a generally good agreement in both epicenter location and focal depth. The latitude difference between the two solutions is approximately 0.10°, while the longitude by about 0.09°. These relatively small horizontal discrepancies indicate that the epicenter location derived from the grid search method is spatially consistent with the BMKG catalog.

In terms of focal depth, the grid search result indicates a depth of 39.00 km, whereas the BMKG catalog reports a depth of 32.4 km, resulting in a depth difference of approximately 6.6 km. This discrepancy may be attributed to differences in the velocity model, phase selection, and earthquake location algorithms employed by each method. The grid search approach adopted in this study utilized a simplified and homogeneous P-wave velocity model, while the BMKG catalog using more complex operational procedures and potentially incorporates additional seismic phases. This depth difference remains within an acceptable range, considering that the depth value reported in the BMKG catalog is based on a fixed depth assumption, wich inherently limis the resolution od source deoth variations. Despite these differences, the RMS residual value of 1.0064 obtained from the grid search analysis suggest that the calculated arrival times reasonably fi the observed P-wave data.

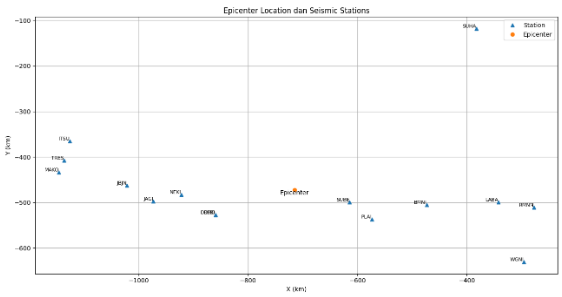

Fig. 2 Distribution of seismic stations and epicenter location

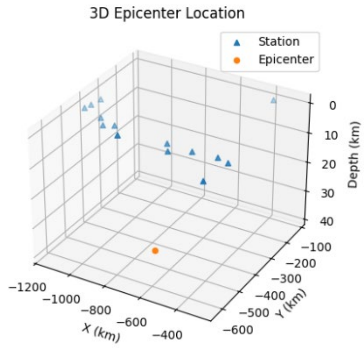

Fig. 3 3D epicenter location

Figure 2 illustrates the horizontal distribution of the 15 accelerometer stations used in this study along with the epicenter location obtained from the grid earch method. The epicenter is located within the coverage of the seismic network, indicating that the station geometry provides sufficient azimuthal control for constraining the earthquake location. This relatively uniform spatial distribution of stations surrounding the epicenter contributes to the small horizontal discrepancies observed in the comparison with the BMKG catalog. This station configuration supports the reliability of the grid search result, particularly in determining the epicenter location, and is consistent with low RMS residual obtained from the arrival time misfit analysis.

The 3d representation of the earthquake source location obtained from the grid search analysis is shown in Figure 3. The figure illustrated the spatial relationship between the seismic station distribution and the estimated hypocenter, with the focal depth located at approximately 39 km beneath the surface network. The 3d visualization provides insight into the vertical geometry of the solution, indicating that the hypocenter is reasonably constrained within the depth range supported by the available P-wave arrival time data.

3.2. RMS Spatial Distribution and Misfit Surface

The RMS heatmap derived from the grid search analysis at the optimal focal depth of 39 km is shown in Figure 4. The heatmap highlights a low RMS region that is elongated in the horizontal direction and centered near the estimated epicenter, indicating that this depth provides the most favorable math between observed and calculated P-wave arrival times. The gradual increase in RMS values away from the low RMS region suggest a smooth spatial variation of the misfit function, implying that horizontal perturbations in the source location lead to systematic changes in RMS values rather than abrupt fluctuations.

The 3d misfit surface derived from the grid search analysis is illustrated in Figure 5. The surface displays a pronounced low RMS region centered near the optimal epicenter location, while RMS values increase gradually away from this region. This smooth variation of RMS values indicates that the misfit function changes continuously with spatial position, suggesting a stable solution rather than one controlled by spurious or isolated local minima. Although the misfit surface exhibits asymmetry in certain directions, the presence of a dominant minimum supports the robustness of the estimated epicenter location.

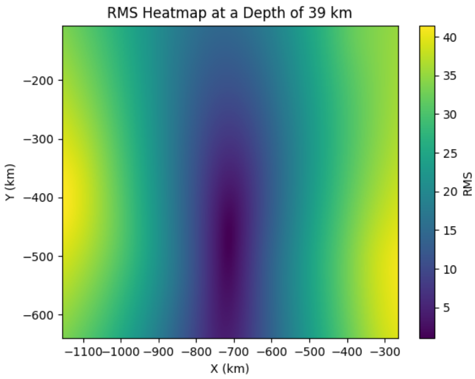

Fig. 4 RMS heatmap at a depth (39 km)

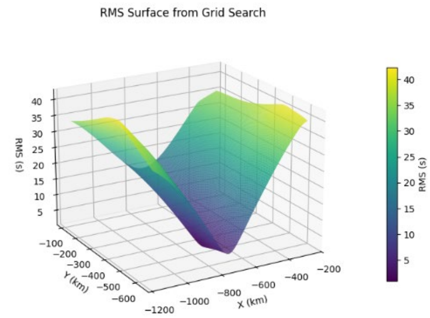

Fig. 5 RMS surface from grid search

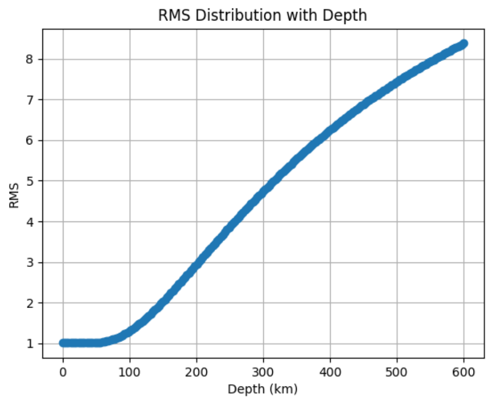

Fig. 6 RMS distribution with depth

The variation of RMS values as a function of depth derived from the grid search analysis is shown in Figure 6. The RMS curve indicates a minimum RMS value at a depth of approximately 39 km, which corresponds to the optimal hypocenter depth obtained in this study. At shallower depths, the RMS values remain relatively low but begin to increase gradually with increasing depth, reflecting a progressive reduction in the fit between observed and calculated P-wave arrival times.

3.3. Seismic Wave Path

The seismic wave paths from the accelerometer stations to the estimated hypocenter derived from the grid search analysis are illustrated in Figure 7. The wave paths were computed assuming a homogeneous P-wave velocity model and represent the theoretical first arrival propagation from the earthquake source to each recording station. The convergence of the wave paths toward the hypocenter indicates that the observed P-wave arrival times recorded at different stations can be consistently explained by a single source location. The variation in ray path orientations reflect the azimuthal distribution of the stations surrounding the epicenter, which contributes to reducing location ambiguity and improving the geometric constraint of the hypocenter.

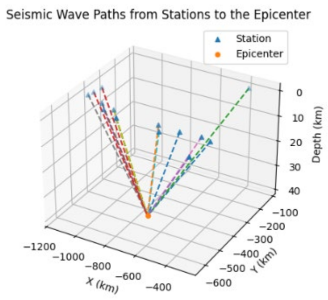

Fig. 7 Seismic wave paths from stations to the Hypocenter

3.3. Travel Time Residual

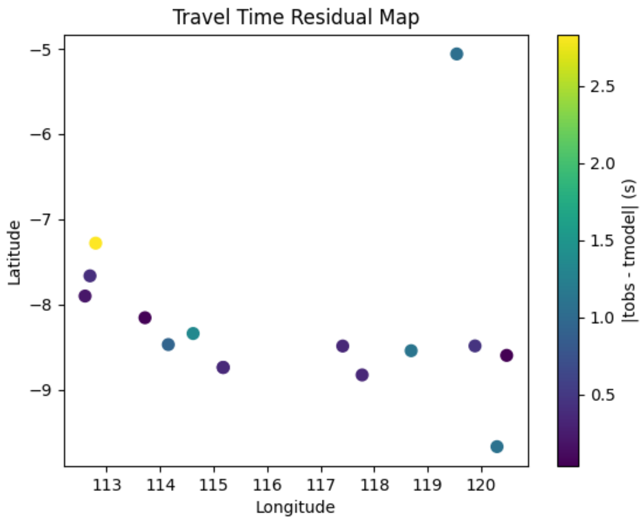

Fig. 8 Travel time residual map

The spatial distribution of P-wave travel time residuals between observed and calculated arrival times is shown in Figure 8. The residual map displays the absolute differences [t_obs- t_model] at each seismic station, represented by color intensity. Most stations exhibit relativel small residual values, generally less than approximately 2 s, indicating a good overall agreement between the observed P-wave arrivals and the travel times predicted by the grid search. A small number of stations show comparatively larger residuals, which are spatially isolated and do not form a systematic pattern across the network. These localized residual variations may be associated with a local site effects, lateral heterogeneities in the crust, or uncertainties in arrival time picking.

4. CONCLUSION

This study applied the grid search method to determine the epicenter and hypocenter of the Mw 7.0 Lombok earthquake that occurred on 5 August 2018 using P-wave arrival time data recorded by 15 accelerometer stations. The grid search analysis yielded a best fit earthquake location at latitude −8.2483°, longitude 116.5566°, a focal depth at 39.00 km, amd a minimum RMS residual of 1.0064 s, indicating a satisfactory fit between observed and calculated arrival times. Comparison with the BMKG catalog shows a generally good agreement in both epicenter location and focal depth. The horizontal discrepancies are relatively small, while the depth difference of approximately 6.6 km remains within an acceptable range, considering that the BMKG catalog employs a fixed depth assumption. Analysis or RMS spatial distributin, 3D misfit surfaces, and RMS variation with depth indicates that the earthquake location is well constrained both horizontally and vertically. The presence of a dominant minimum in the misfit function, together with the smooth variation of RMS values, suggest that the obtained solution is stable and not influenced by spurious local minima. Overall, the results confirm that the grid search method is an effective and robust approach for earthquake location analysis in tectonically complex regions such as Lombok Island.

REFERENCE

[1] S. J. Hutchings and W. D. Mooney, “The Seismicity of Indonesia and Tectonic Implications Geochemistry, Geophysics, Geosystems,” pp. 1–42, 2021, doi: 10.1029/2021GC009812.

[2] H. Afif et al., “Local earthquake tomography of the source region of the 2018 Lombok earthquake sequence , Indonesia,” pp. 1814–1823, 2021.

[3] P. M. Shearer, “Improving local earthquake locations using the L1 norm and waveform cross correlation: Application to the Whittier aftershock sequence Narrows California,” vol. 102, no. 134, pp. 8269–8283, 1997.

[4] S. Husen, E. Kissling, N. Deichmann, S. Wiemer, D. Giardini, and M. Baer, “Probabilistic earthquake location in complex 3d velocity models : Application to Switzerland,” vol. 108, no. February, 2003, doi: 10.1029/2002JB001778.

[5] H. Gökalp, “Estimation of Hypocentral Paremeters of Local / regional Earthquakes by Grid Search Method With a Fuzzy Logic Approach,” pp. 0–42, 2024.

[6] H. Nugroho, S. Widiyantoro, and A. D. Nugraha, “Hypocenter Relocation using a Fast Grid Search Method and a 3-D Seismic Velocity Model for the Sumatra Region,” vol. 293, no. 2013, pp. 10–14, 2015, doi: 10.1063/1.4820343.